Journal of Power Sources 184 (2008) 527–531

Contents lists available at ScienceDirect

Journal of Power Sources

journal homepage: www.elsevier.com/locate/jpowsour

Short communication

Surface-modified maghemite as the cathode material for lithium batteries

James Manuel [a], Jae-Kwang Kim [a], Jou-Hyeon Ahn [a,*], Gouri Cheruvally [c], Ghanshyam S. Chauhan [a], Jae-Won Choi [a], Ki-Won Kim [b]

[a] Department of Chemical and Biological Engineering and Engineering Research Institute, Gyeongsang National University, 900 Gajwa-dong, Jinju 660-701, Republic of Korea
[b] School of Nano and Advanced Materials Engineering and Engineering Research Institute, Gyeongsang National University, 900 Gajwa-dong, Jinju 660-701, Republic of Korea
[c] Polymers and Special Chemicals Division, Vikram Sarabhai Space Centre, Thiruvananthapuram, Kerala, India

ARTICLE INFO

Article history:
Received 21 December 2007
Received in revised form 22 February 2008
Accepted 27 February 2008
Available online 6 March 2008

Keywords:
Maghemite
Cathode material
Lithium batteries
Inorganic–organic hybrid
Polypyrrole

ABSTRACT

The inorganic–organic hybrid maghemite (γ-Fe_2O_3)/polypyrrole (PPy) was synthesized and evaluated as cathode-active material for room temperature lithium batteries. The nanometer-sized core–shell structure of the hybrid consisting of the maghemite core with surface modified by PPy was evidenced from the morphological examination. The cathode fabricated with the as-prepared hybrid material delivered an initial discharge capacity of 233 mAh g^{-1} and a reversible capacity of ~62 mAh g^{-1} after 50 charge–discharge cycles. A much higher performance with an initial discharge capacity of 378 mAh g^{-1} and a reversible capacity of ~100 mAh g^{-1} was achieved with the cathode based on the segregated active material, which was obtained by subjecting the as-prepared hybrid material to an additional ball-milling process. The study demonstrates the promising lithium insertion characteristics of the nanometer-sized core–shell maghemite/PPy particles prepared under optimized conditions for application in secondary batteries.

1. Introduction

The field of advanced power sources is presently dominated by the lithium battery technology that caters to a multitude of applications. A lot of research work is being carried out for developing promising cathode materials for lithium batteries. Although satisfactory discharge capacity and stable cycle life are provided by $LiCoO_2$, there is an increasing demand to replace it by other suitable cathode materials that are non-toxic, inexpensive and more easily available. Sulfur and iron-based compounds which meet these criteria are thus very attractive.

Several iron compounds have attracted interest as cathode materials including iron oxides, sulfides and mixed metal oxides like $LiFeO_2$ and $LiFePO_4$. Among these, the iron oxides are particularly attractive from cost and environmental stand points. However, the initial studies with the micrometer-sized crystalline iron oxide as lithium intercalation electrodes were not reported to be promising, because of its poor conductivity [1–4]. Nanostructured cathode materials such as V_2O_5 [5] and $LiMn_2O_4$ [6] were reported to exhibit enhanced electrochemical performance compared to their micrometer-sized counterparts. There are many reports on the electrochemical performance of the nano-structured iron oxide materials [7–14]. Xu et al. reported that nano-crystalline Fe_2O_3 with a structure resembling that of α-Fe_2O_3 exhibited better Li intercalation properties with improved cyclability compared to the micro-crystalline α-Fe_2O_3 [8]. The enhanced properties of the nano-structured cathodes result from the higher surface area of the active material, shorter diffusion paths for lithium ions and only small dimensional changes go through the particles on cycling. In addition, the structural defects at/near the surface of the nanocrystalline materials lead to many sub-band gap states between the conduction and valance bands, and result in a better adaptation to the structural changes, as reported by Kwon et al. [15].

Maghemite (γ-Fe_2O_3) is an important crystalline form of Fe(III) oxide. Its nanoparticles have been prepared by different synthetic methods [16,17]. The lithium intercalation property of the pristine maghemite is not so attractive mainly due to its low electrical conductivity. Kwon et al. achieved enhanced electrochemical performance using nano-sized core–shell particles of the inorganic–organic hybrid of γ-Fe_2O_3/polypyrrole (PPy), which was prepared by the surface modification of γ-Fe_2O_3 with PPy [15,18]. PPy forms a thin layer over the maghemite particles that facilitates easy transport of electrons and ions, and thus enhances the capacity and cyclability of the cell. In the present study, we report the prepa-

* Corresponding author. Tel.: +82 55 751 5388; fax: +82 55 753 1806.
E-mail address: jhahn@gsnu.ac.kr (J.-H. Ahn).

0378-7753/$ – see front matter © 2008 Elsevier B.V. All rights reserved.
doi:10.1016/j.jpowsour.2008.02.079

ration of segregated nanoparticles of γ-Fe_2O_3/PPy hybrid material by adopting an additional ball-milling process. This material exhibited enhanced performance when evaluated as cathode in lithium batteries operating at room temperature.

2. Experimental

Maghemite nanoparticles were prepared by a minor modification of the method reported by Massart et al. [16,17]. All chemicals (from Aldrich) were used as received. 14.3 ml aqueous solution of 2.21 M $FeCl_3$ (containing 31.6 mmol of $FeCl_3$) and 17 ml of 1.5 M HCl containing 3.14 g $FeCl_2$ (15.8 mmol $FeCl_2$), were added to 350 ml water and heated up to 50 °C. To this, 34.73 g NH_4OH solution in 30 ml water was added drop-wise under vigorous stirring to yield magnetite (Fe_3O_4). The solution was decanted and washed to remove ammonia, and the Fe_3O_4 particles (yield 3.6 g) were collected after removing the residual solvents by rotary evaporation at ~70 °C for 2 h. The product was acidified and oxidized by HNO_3 and $Fe(NO_3)_3$ to yield maghemite, which was washed several times with water and followed by washing with acetone and dried at 40 °C.

2.0 g of maghemite was taken in a watch glass and the surface of the particles was made homogenously wet with 1.53 g of liquid pyrrole (Py) added using a micropipette. This quantity of Py was found to be just sufficient for the complete wetting of the maghemite particle surface. The Py molecules were subsequently polymerized. For this, the mixture was added to 200 ml ethanol solution of 0.15 M $FeCl_3$ under stirring and the reaction was continued for 6 h. Maghemite/PPy hybrid material being magnetic was separated from the non-magnetic bare PPy by adopting the magnetic method. The hybrid particles settled at the bottom, while the upper layer of PPy was removed by repeated washing with ethanol and acetone. Fourier transform infrared (FTIR) spectra was recorded using VERTEX 80v (Bruker Optics) spectrometer. Surface morphology was studied using scanning electron microscopy (SEM: Philips XL 30 S FEG and JEOL JSM-5600) and transmission electron microscopy (TEM: JOEL JEM-2010) operating at an acceleration voltage of 200 kV. Elemental analysis was carried on CHNS-932 (LECO) and thermogravimetric analysis (TGA) was performed in argon at a heating rate of 10 °C min^{-1} in the temperature range 30–900 °C on a thermobalance model SDT Q600, TA (USA) using Pt crucibles.

The positive electrode was prepared by mixing the hybrid maghemite/PPy active material with conductive agent carbon black (Super-P) and binder poly(vinylidene fluoride) (PVdF) in 75:15:10 weight ratio. The ingredients were mixed together in *N*-methylpyrrolidone (NMP) solvent in a high energy mixer mill at room temperature for 45 min to get homogeneous slurry which was cast on aluminum foil and dried under vacuum at 80 °C for 24 h to get the film of ~23 μm thickness. The film was cut into circular discs of area 0.95 cm^2 and mass ~3.5 mg for use as the cathode. Since the nanoparticles of maghemite/PPy hybrid might have a tendency to agglomerate, we prepared another set of cathode based on a segregated sample of the active material. The maghemite/PPy particles were subjected to ball-milling for 2 h at 1080 rpm in NMP solvent at room temperature followed by evaporation to remove the solvent. In the ball-milling process, a ball-to-powder ratio of 2:1 was employed using zirconia balls with a diameter of 5.1 mm in a hardened steel jar.

Two-electrode electrochemical coin cells were assembled with lithium metal (300 μm thickness, Cyprus Foote Mineral Co.) as anode, Celgard®2200 separator, 1 M $LiPF_6$ in ethylene carbonate (EC)/dimethyl carbonate (DMC) (1:1, v/v) electrolyte and maghemite/PPy as cathode. The lithium salt and organic solvents were supplied by Aldrich. The cell assembly was performed under argon atmosphere in a glove box with H_2O level <10 ppm. Cyclic voltammetry (CV) was done at a scan rate of 0.3 mV s^{-1} between 1.5 and 4.0 V. Electrochemical performance tests were carried out using an automatic galvanostatic charge–discharge unit, WBCS3000 battery cycler, between 1.5 and 4.0 V at room temperature. The experiments were performed at a current density corresponding to 0.1 C (0.066 mA cm^{-2}).

3. Results and discussion

The nano-sized particles of the maghemite/PPy hybrid material have been confirmed by morphological observations (Fig. 1). The SEM image shows that the hybrid material is made up of spherical particles which have a tendency to agglomerate. The core–shell nature of the hybrid material is not clear from the SEM image of the sample taken at a lower magnification (scale of 1 μm). A better analysis is given by the TEM images in Fig. 1(b) and (c) at 100 and 20 nm scales, respectively. The individual particles are spherical in shape with a particle size of ~10 nm. The bright regions between the darker spheres represent PPy coating over the maghemite particles. The clear lattice images of the crystalline γ-Fe_2O_3 particles seen in TEM reveal that the core structures of the maghemite nanoparticles remain unchanged, while the surfaces is modified with PPy. A similar observation has been made by Kwon et al. also in an earlier study on the hybrid material [18]. The segregation of the particles is evident from the TEM image of the ball-milled hybrid particles (Fig. 1d). It is also evident that the ball-milling does not affect the PPy coating on the particles.

Elemental analysis of the maghemite/PPy hybrid materials was done to determine the amount of PPy coated on the maghemite. PPy was calculated to be 12.0% and 12.5% for the as-prepared and balled hybrid materials, respectively, from the nitrogen content. The thermal degradation of PPy is a three-stage process (Fig. 2). From the TGA curves it is apparent that in both the samples all the PPy is lost before ~600 °C. From these curves, the weight loss ascribed to PPy decomposition corresponds to nearly 11% for both samples, i.e., in close agreement with the amount of the PPy obtained from the elemental analysis. The shape of the curves up to 600 °C is similar to that has been reported in an earlier study for PPy coated on γ-Fe_2O_3 [19].

FTIR spectra of maghemite/PPy hybrid material are presented in Fig. 3. The spectra have the characteristic peaks of both maghemite and PPy. The peaks in the 400–800 cm^{-1} region (443, 588, 630 and 792 cm^{-1}) are due to the multiple lattice absorptions of the partially ordered maghemite [20]. The main characteristic peaks of PPy were assigned as follows: the bands at 1620 [N–H bending], 1562 and 1465 cm^{-1} [C=C stretching] and those at 1303 and 1100 cm^{-1} due to the =C–H in-plane deformation, and the band at 1049 cm^{-1} due to C–N stretching vibration [21–24]. The broad band at 3430 cm^{-1} is due to the NH stretching [24].

The positive electrode was fabricated by blending the active material with conductive carbon powder (of approximate size 40 nm) and PVdF binder. The cathode so prepared has a fairly uniform morphology indicating a homogeneous mixing of the ingredients in the preparation process (Fig. 4). The utilization of the active material as electrode in a battery is highly dependent on the particle size and the uniformity of particle size distribution. Since the maghemite/PPy hybrid particles show a tendency to get agglomerated because of their nanometer particle size, an additional processing step of ball-milling was undertaken to segregate the particles. Thus, the electrochemical performance studies were performed with two types of cathodes fabricated with the as-prepared and ball-milled active materials, respectively. Fig. 5(a) shows the first cycle CV curves of the cells at room temperature between 1.5 and 4.0 V. A multi-step redox process seems to be operating for the maghemite/PPy cathode material with anodic peaks

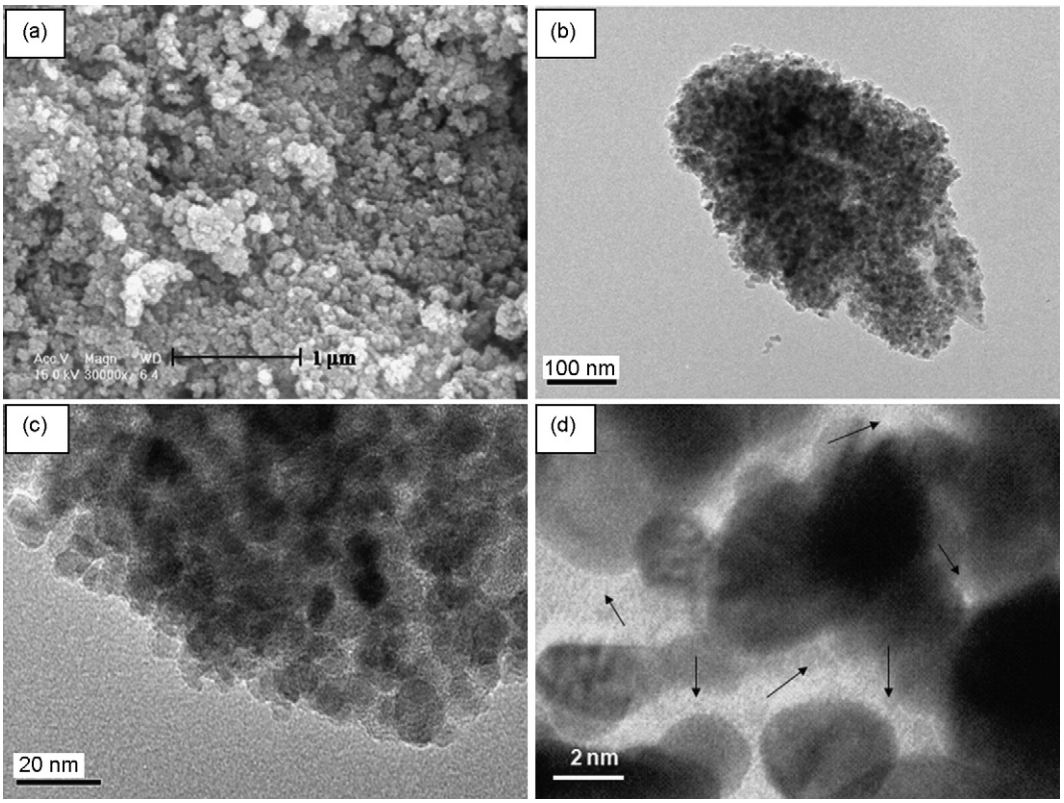

Fig. 1. (a) SEM image; (b) and (c) TEM images of as-prepared maghemite/PPy hybrid material at different magnifications; (d) TEM image of ball-milled maghemite/PPy hybrid material.

centered at 2.3 and 3.0 V, and cathodic peaks centered at 2.5 and 1.5 V. The CV curve of the ball-milled material exhibits more conspicuous oxidation and reduction peaks with the higher current as compared to the as-prepared material. This is attributed to the enhanced electrochemical activity of the ball-milled, segregated particles. The segregation of particles results in the exposure of larger area of the surface of the active material. It also lowers distance for the lithium ion and electron to diffuse during the redox process. Further, PPy coating improves electronic conductivity of the material. The CV curves thus indicate a better charge–discharge performance of the cell based on the ball-milled hybrid material. During repeated cycling, the CV curves follow almost the same pattern, as shown in Fig. 5(b), for the ball-milled material showing good reversibility of the redox process.

The first step in utilizing nano-structured maghemite as a cathode material in lithium battery is lithium insertion into its structure. As reported in earlier studies, lithium insertion begins with the electrochemical grafting of lithium ions, which is promoted by the structural defects at/near the nanocrystalline surface [15]. The process of electrochemical lithium insertion into maghemite having a defective spinel structure has been reported in earlier studies [18,25]. The process starts with the filling of octahedral vacancies in the structure. This is followed by a plateau at ~2.7 V due to the structural transformation into a layered rock-salt like structure and lithium insertion into 16*c* sites. This involves a major rearrangement of 8*a* tetrahedral Fe^{3+} ions to the 16*c* octahedral sites. Finally the lithium ions enter the remaining 16*c* sites with a drop in voltage to 1.3 V. Thus, the discharge process of pristine

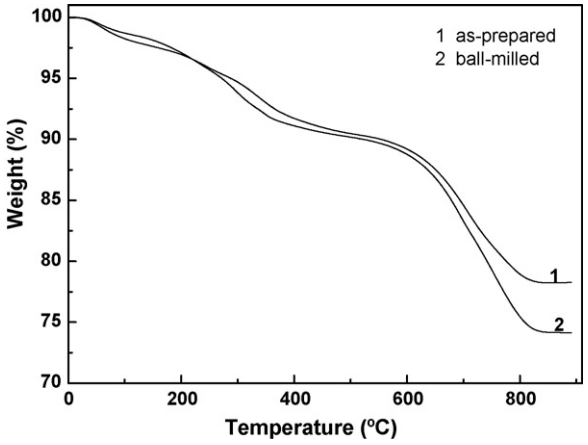

Fig. 2. TGA curves of as-prepared and balled-milled maghemite/PPy hybrid materials.

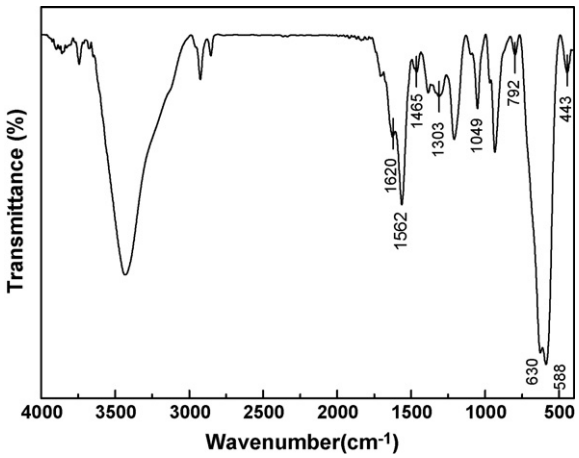

Fig. 3. FTIR spectra of maghemite/PPy hybrid material.

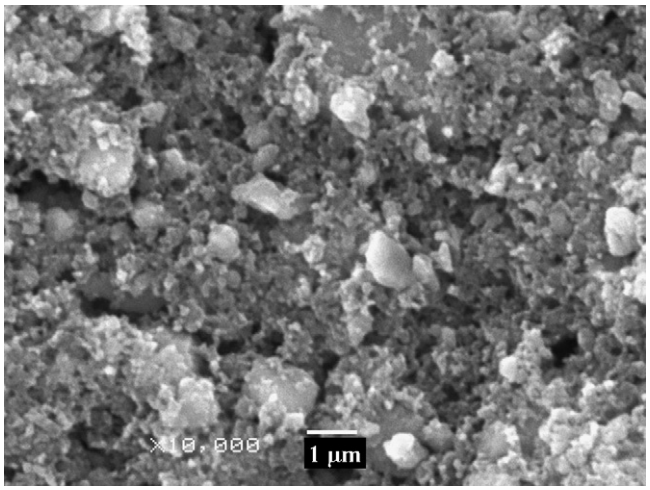

Fig. 4. SEM image of the composite cathode based on ball-milled maghemite/PPy hybrid.

maghemite showed a distinctive voltage plateau at 2.7 V in these studies. In contrast, when maghemite/PPy hybrid is used as the active material, the potential decrease is smooth with a less obvious discharge plateau at 2.7 V [15,18]. A similar observation is also made in the present study. Thus, nearly smooth charge–discharge curves for the first cycle are obtained for the lithium cell with the core–shell hybrid cathode, as shown in Fig. 6. This difference in behavior between pristine maghemite and maghemite/PPy hybrid

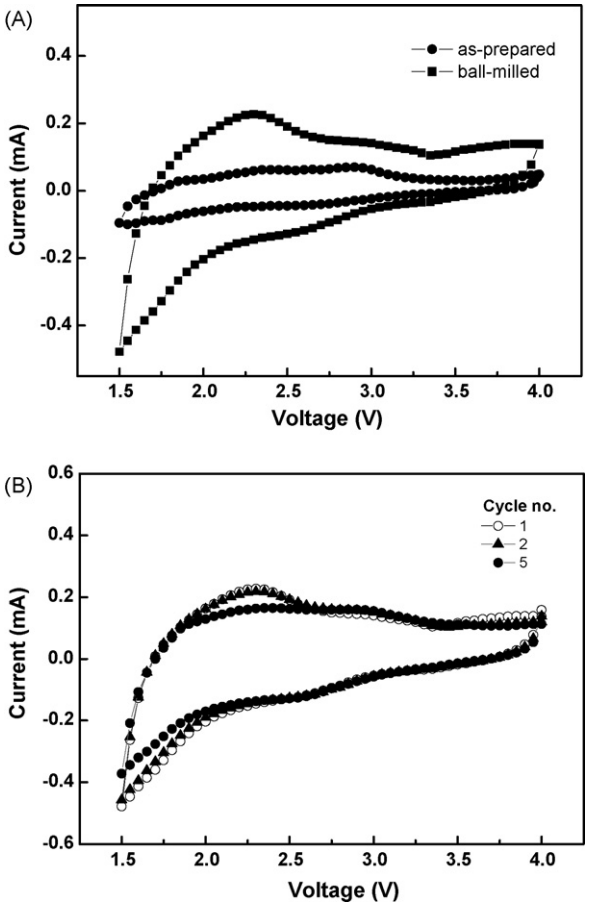

Fig. 5. (a) CV curves during the first cycle of as-prepared and ball-milled maghemite/PPy hybrids and (b) CV curves during cycling of ball-milled maghemite/PPy hybrid (0.3 mV s^{-1}, 25 °C, 1.5–4.0 V).

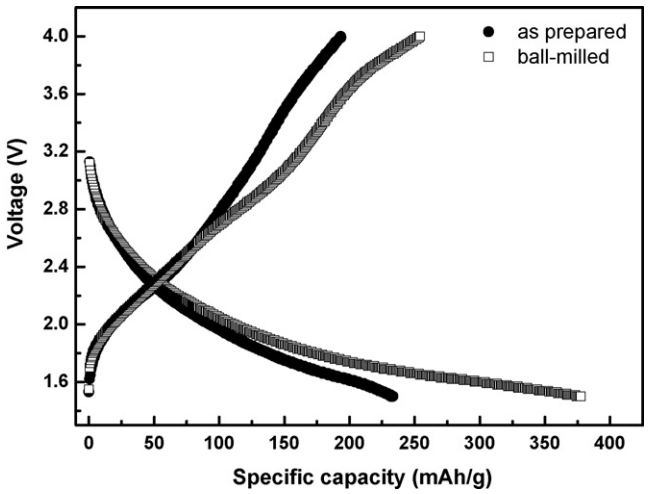

Fig. 6. Specific capacity curves for the first cycle of lithium cells based on as-prepared and ball-milled maghemite/PPy hybrids as cathode materials (25 °C, 1.5–4.0 V, 0.1 C-rate).

material is an indication of the change in the electrical properties of the material brought about by the surface modification [18]. The as-prepared hybrid material delivers a first cycle discharge capacity of 233 mAh g^{-1} corresponding to the insertion of 1.38 mol of lithium per mole of Fe_2O_3. The segregated sample of maghemite/PPy hybrid material delivers a still higher discharge capacity of 378 mAh g^{-1}, which is 1.6 times that of the as-prepared sample. The discharge capacity delivered by the cell during the first cycle at 0.1 C-rate corresponds to the insertion of 2.25 mol of lithium per mol of Fe_2O_3. This shows the availability of higher reaction sites in the ball-milled sample and the more effective transfer of charges taking place at the electrode, as has been observed in the CV studies also.

The performance of the cells on repeated charge–discharge cycling at 0.1 C-rate is shown in Fig. 7. There is a fast decrease in the specific capacity during the initial cycles, especially up to 5 cycles, thereafter the capacity decreases slowly and then tends to stabilize after ~20 cycles. The cell with the ball-milled maghemite/PPy hybrid as the active material exhibits a discharge capacity of 103 mAh g^{-1} after 50 cycles, which is ~80% of the capacity attained after 20 cycles, 128 mAh g^{-1}. The mismatch between the charge and discharge capacities is high during the initial cycles showing irreversible loss of the active material. However, the difference in the values gets closer as the cycling progresses and a coulombic efficiency >90% is attained after ~8 cycles. Thus, the

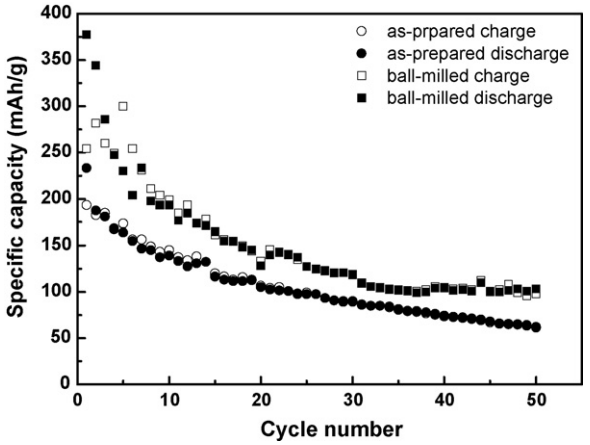

Fig. 7. Cycle performance of lithium cells based on as-prepared and ball-milled maghemite/PPy hybrids as cathode materials (25 °C, 1.5–4.0 V, 0.1 C-rate).

cell with the cathode based on ball-milled maghemite/PPy hybrid material shows a stable and reversible capacity of ~100 mAh g^{-1}. A similar trend in cycle performance is exhibited by the cell based on the as-prepared maghemite/PPy hybrid material as cathode, but delivers a lower specific capacity. This cell has a discharge capacity of 105 mAh g^{-1} after 20 cycles and 62 mAh g^{-1} after 50 cycles. The comparison shows that the segregation of the agglomerated nanoparticles of maghemite/PPy hybrid material improves its electrochemical performance which leads to a reversible capacity for the cell that is ~1.6 times greater than that of the material based on the agglomerated hybrid.

4. Conclusions

The inorganic–organic hybrid material of maghemite/PPy has been synthesized as particles of ~10 nm size with the core structure of Fe_2O_3 remaining intact and the surface being modified with PPy. The particles show electrochemical activity characteristic of nano-sized Fe_2O_3 when evaluated in lithium metal batteries at room temperature at 0.1 C-rate. An initial discharge capacity of 233 mAh g^{-1} corresponding to 1.38 mol of lithium per mol of Fe_2O_3 is obtained with the as-prepared material-based cathode. For enhancing the performance, the material was subjected to a high energy ball-milling step which segregates the agglomerated particles leading to an increase in the surface area and a shortening of the ion and electron diffusion lengths. The cell based on the segregated active material as cathode delivered an initial discharge capacity of 378 mAh g^{-1} and a stable and reversible capacity of ~100 mAh g^{-1} after 50 cycles. The study shows that the surface-modified nano-sized maghemite particles prepared under optimized conditions could serve as a low cost, yet efficient cathode material for lithium batteries with satisfactory performance at the low current densities.

Acknowledgements

This research was supported by Ministry of Knowledge Economy, Korea, under the Information Technology Research Center (ITRC) support program supervised by the Institute of Information Technology Assessment (IITA).

References

[1] M. Pernet, P. Strobel, B. Bonnet, P. Bordet, Solid State Ionics 66 (1993) 259.
[2] M.M. Thackeray, W.I.F. David, J.B. Goodenough, Mater. Res. Bull. 17 (1982) 785.
[3] M. Pernet, J. Rodriguez, M. Gonderand, J. Fontcuberta, P. Strobel, J.C. Joubert, Proceedings of ICF-5, India, 1989.
[4] B. Bonnet, P. Strobel, M. Pernet, M. Gonderand, Y. Gros, C. Mouget, Y. Chaber, Mater. Sci. Forum 91–93 (1992) 345.
[5] A. Singal, G. Skandan, G. Amatucci, N. Pereira, in: A.R. Landgrebe, R.J. Klinger (Eds.), Electrochem. Soc. Proceedings, vol. 2000-36, 2001, p. 244.
[6] S.-H. Kang, J.B. Goodenough, L.K. Rabenberg, Chem. Mater. 13 (2001) 1758.
[7] S. Kanzaki, T. Inada, T. Matsumura, N. Sonoyama, A. Yamada, M. Takano, R. Kanno, J. Power Sources 146 (2005) 323.
[8] J.J. Xu, G. Jain, Electrochem. Solid State Lett. 6 (2003) A190.
[9] D. Larcher, D. Bonnin, R. Cortes, I. Rivals, L. Personnaz, J.-M. Tarascon, J. Electrochem. Soc. 150 (2003) A1643.
[10] D. Larcher, C. Masquelier, D. Bonnin, Y. Chabre, V. Masson, J.-B. Leriche, J.-M. Tarascon, J. Electrochem. Soc. 150 (2003) A133.
[11] T. Matsumura, N. Sonoyama, R. Kanno, M. Takano, Solid State Ionics 158 (2003) 253.
[12] S. Komaba, K. Suzuki, N. Kumagai, Electrochemistry (Tokyo, Japan) 70 (2002) 506.
[13] S. Ito, K. Ui, N. Koura, K. Akashi, Solid State Ionics 113–115 (1998) 17.
[14] S. Ito, T. Aoyama, K. Akashi, Solid State Ionics 113–115 (1998) 23.
[15] C.W. Kwon, M. Quintin, S. Mornet, C. Barbieri, O. Devos, G. Campet, M.H. Delville, J. Electrochem. Soc. 151 (2004) A1445.
[16] R. Massart, IEEE Trans. Magn. 17 (1981) 1247.
[17] R. Massart, S. Neveu, V. Cabuil-Marchal, R. Brossel, J. M. Fruchart, T. Bouchami, J. Roger, A. Bee-Debras, J.N. Pons, M. Carpentier, French Patent No. 2662539 (1990).
[18] C.W. Kwon, A. Poquet, S. Mornet, G. Campet, J. Portier, J.H. Choy, Electrochem. Commun. 4 (2002) 197.
[19] K. Sunderland, P. Brunetti, L. Spinu, J. Fang, Z. Wang, W. Lu, Mater. Lett. 58 (2004) 3136.
[20] M.P. Morales, S.V. Verdaguer, M.I. Montero, C.J. Serna, A. Roig, L. Casas, B. Martinez, F. Sandiumenge, Chem. Mater. 11 (1999) 3058.
[21] H.V.R. Dias, M. Fianchini, R.M.G. Rajapakse, Polymer 47 (2006) 7349.
[22] M.V. Murugendrappa, A. Parveen, M.V.N.A. Prasad, Mater. Sci. Eng. A 459 (2007) 371.
[23] H. Mi, X. Zhang, X. Ye, S. Yang, J. Power Sources 176 (2007) 403.
[24] H.C. Kang, K.E. Geckeler, Polymer 41 (2000) 6931.
[25] M. Pernet, P. Strobel, B. Bonnet, P. Bordet, Y. Chabre, Solid State Ionics 66 (1993) 259.